Mechanisms that Specify Promoter Nucleosome Location and Identity

Paul D. Hartley[1] and Hiten D. Madhani[1,*]

[1]Department of Biochemistry and Biophysics, University of California, San Francisco, 600 16th St.. MC2200, San Francisco, CA 94158, USA
*Correspondence: hitenmadhani@gmail.com
DOI 10.1016/j.cell.2009.02.043

SUMMARY

The chromatin architecture of eukaryotic gene promoters is generally characterized by a nucleosome-free region (NFR) flanked by at least one H2A.Z variant nucleosome. Computational predictions of nucleosome positions based on thermodynamic properties of DNA-histone interactions have met with limited success. Here we show that the action of the essential RSC remodeling complex in *S. cerevisiae* helps explain the discrepancy between theory and experiment. In RSC-depleted cells, NFRs shrink such that the average positions of flanking nucleosomes move toward predicted sites. Nucleosome positioning at distinct subsets of promoters additionally requires the essential Myb family proteins Abf1 and Reb1, whose binding sites are enriched in NFRs. In contrast, H2A.Z deposition is dispensable for nucleosome positioning. By regulating H2A.Z deposition using a steroid-inducible protein splicing strategy, we show that NFR establishment is necessary for H2A.Z deposition. These studies suggest an ordered pathway for the assembly of promoter chromatin architecture.

INTRODUCTION

Since the identification of a nucleosome-free region (NFR) in SV40 minichromosomes nearly 30 years ago (Jakobovits et al., 1980; Saragosti et al., 1980), the mechanisms underlying the positioning of nucleosomes have been an area of active study. Recent genome-scale surveys of nucleosome positions in a variety of eukaryotic organisms have revealed a stereotypical promoter chromatin architecture characterized by a nucleosome-free region (NFR) flanked by at least one nucleosome enriched for the histone H2A variant H2A.Z (Albert et al., 2007; Lee et al., 2007; Mavrich et al., 2008a; Mavrich et al., 2008b; Ozsolak et al., 2007; Raisner et al., 2005; Yuan et al., 2005). As a class, NFR-adjacent nucleosomes are the most precisely positioned in the genome, with neighboring nucleosomes displaying less precision in their locations as their distance from NFRs increases. By acting as anchor points, the tight positioning of NFR-flanking nucleosomes may be a dominant mechanism by which nucleosomes are positioned genome-wide (Mavrich

et al., 2008a). In *S. cerevisiae*, NFR-flanking nucleosomes often occlude the transcription start site (TSS) such that the TSS is on average half a helical turn inside the +1 nucleosome and exhibits a rotational phasing which tends to place sites for transcription factors on the accessible surface of nucleosomal DNA (Albert et al., 2007). Significantly, recent detailed analysis of the *PHO* regulon in *S. cerevisiae* has shown that chromatin remodeling during phosphate starvation exposes a class of binding sites for the Pho4 activator that are initially masked by nucleosomes and that this plays a key role in shaping the input-output functions of promoters (Lam et al., 2008). Defects in the positioning of some promoter nucleosomes seen in *isw2* mutant cells correlates with the accumulation of cryptic antisense transcripts, leading to the proposal that positioning of nucleosomes also prevents erroneous transcription initiation events (Whitehouse et al., 2007).

While the fractional occupancy of H2A.Z in NFR-flanking nucleosomes in yeast is not correlated with transcription rates (Raisner et al., 2005), loss of promoter nucleosomes including those containing H2A.Z occurs in response to transcriptional activation (Bernstein et al., 2004; Schones et al., 2008; Shivaswamy et al., 2008; Zanton and Pugh, 2006). It has been reported that H2A.Z nucleosomes are less stable in vitro, and this property has been hypothesized to aid in their removal in vivo (Zhang et al., 2005). In *Drosophila* and humans, NFRs flanked by nucleosomes enriched in H2A.Z are also a common feature of promoters (Barski et al., 2007; Mavrich et al., 2008b). In flies, the H2A.Z nucleosomes at promoters tend to occur downstream of the NFR, whereas in humans there appear to be H2A.Z nucleosomes both upstream and downstream of NFRs. Interestingly, both NFR formation and H2A.Z deposition seem to correlate with productive transcription in these organisms. These species-specific differences suggest additional complexity in metazoans. H2A.Z nucleosomes are also relatively enriched at flanking non-promoter NFRs that characterize enhancers and insulators in human T cells (Barski et al., 2007). Taken together, nucleosome-free regions, whether or not associated with gene promoters, tend to be associated with H2A.Z. A conserved function of H2A.Z demonstrated in both *S. cerevisiae* and *Arabidopsis thaliana* is to act in euchromatin to antagonize gene silencing (Meneghini et al., 2003; Zilberman et al., 2008).

Despite the high conservation across eukaryotic evolution of these basic aspects of promoter chromatin architecture identified by descriptive genomic studies, the mechanisms by which NFRs flanked by H2A.Z nucleosomes form remain poorly understood. There exists evidence that octamer positioning

genome-wide is mediated by a genomic nucleosome positioning code in which intrinsic DNA-octamer affinities, predicted computationally based on dinucleotide periodicity patterns and/or other sequence patterns, are a significant determinant of location, particularly at NFR-flanking nucleosomes (Ioshikhes et al., 2006; Lee et al., 2007; Segal et al., 2006). For example, one study (Segal et al., 2006) reported that 50% of nucleosome positions in *S. cerevisiae* chromosome III can be accurately predicted computationally. However, there are differences of opinion in the literature regarding how well computational methods predict actual positions determined experimentally compared to so-called random guess predictions (Peckham et al., 2007; Segal, 2008; Yuan and Liu, 2008). A recent study (Yuan and Liu, 2008) compared a number of methods and found that for *S. cerevisiae* datasets even improved methods required an error of ~70bp (nearly half a nucleosome) to obtain a prediction sensitivity of 80% and required a similar error to yield an specificity of 80%. These errors stand in contrast to the observed precision of nucleosome positioning in vivo relative to TSSs and transcription factor-binding sites as described above.

The connection between NFR formation and H2A.Z deposition is likewise not well-defined. One report suggested that H2A.Z deposition plays a role in nucleosome positioning, while another proposed that H2A.Z deposition has no role (Guillemette et al., 2005; Li et al., 2005). H2A.Z nucleosomes have been reported to be poor in vitro substrates of chromatin remodeling enzymes compared to their H2A counterparts (Li et al., 2005). Thus, whether NFR formation is required for H2A.Z deposition or vice versa is unknown.

In the absence of a consensus view of how promoter chromatin architecture is specified with precision, we sought to clarify the underlying mechanisms. In previous work, we identified a segment of the *SNT1* promoter required for normal levels of H2A.Z deposition. Remarkably, insertion of a short segment of this region into the middle of a transcriptionally quiescent *PRM1* gene resulted in the formation of an NFR flanked by two nucleosomes containing H2A.Z (Raisner et al., 2005). This sequence contained a putative binding site for the Myb family transcription factor Reb1 and an adjacent T tract. Below we describe further studies of this synthetic NFR as well as chromosome-wide studies of the roles of several essential factors in nucleosome positioning and H2A.Z deposition.

RESULTS

Models for NFR Formation and H2A.Z Deposition

We considered three models by which the DNA signal containing the Reb1-binding motif (henceforth called Reb1:dT$_7$) might program promoter chromatin structure (Figures 1A and 1B). In Model I, the DNA signal first programs NFR formation, and then the NFR acts as a signal to induce H2A.Z deposition into the flanking nucleosomes. Model II proposes the reverse process of NFR formation such that a DNA signal first induces H2A.Z deposition, and H2A.Z then acts as a signal for NFR formation. Lastly, NFR formation and H2A.Z deposition could occur in an independent, uncoupled fashion (Model III). To distin-

guish these models, we first sought to define *trans*-acting factors that mediate NFR formation.

Construction of Conditional Degron Alleles of Reb1, Abf1, and the RSC ATPase Sth1

The mechanism by which Reb1:dT$_7$ induces formation of an NFR flanked by two nucleosomes carrying H2A.Z likely involves the recruitment of Reb1, although this was not tested directly in our previous study. We also hypothesized that Reb1 might recruit a chromatin remodeling enzyme to produce an NFR. A systematic study of protein interactions revealed that Reb1 physically associates with Rsc2, Rsc3 and Npl6, which are subunits of the essential chromatin remodeling complex RSC (Cairns et al., 1996, 1999; Gavin et al., 2002). Since the Reb1-related factor, Abf1, has also been implicated in the formation of a nuclease-sensitive site (De Winde et al., 1993), we pursued its functional role.

As Reb1, Abf1, and the catalytic subunit of RSC (Sth1) are all essential proteins, we generated a series of conditional alleles Specifically, we used the temperature-sensitive degron system to engineer yeast strains in which we could control degradation of these proteins via the N-end rule pathway (Dohmen and Varshavsky, 2005). This pathway operates through the recognition of destabilizing N-terminal amino acids by the nonessential E3 ubiquitin ligase Ubr1. A N-terminal arginine is the strongest signal for degradation by Ubr1, and traditional degron alleles encode proteins capped by an arginine followed by a temperature-sensitive murine dihydrofolate reductase (DHFR^{ts}) peptide fused to the target protein. Because translation initiates at an ATG codon, an ATG-initiated segment encoding a ubiquitin moiety is placed before the arginine codon. Once synthesized, this segment is cleaved in cells by ubiquitin C-terminal proteases to expose the N-terminal arginine. Such degron systems also place the modified allele of interest under the control of a regulatable promoter, which traditionally has been the copper-inducible promoter *pCUP1*.

We constructed *pCUP1::UBI4::DHFR^{ts}::c-myc::STH1* and *pCUP1::UBI4::DHFR^{ts}::c-myc::REB1* alleles in strains that had *UBR1* under the control of the *pGAL1* promoter. We were unable to achieve substantial degradation of these proteins or growth arrest under degron-inducing conditions, although such an allele for *STH1* has been reported (Parnell et al., 2008). We achieved more complete degradation of Reb1 and Sth1 under degron-inducing conditions with a different construct (*pMET3::UBI4::DHFR^{ts}::3xHA*) that utilized the methionine-repressed *pMET3* promoter (Figure 1C). Yeast strains carrying Reb1-degron or Sth1-degron alleles were inviable under degron-inducing conditions (Figure 1D). While an Abf1 DHFR^{ts} degron has been reported in the W303 strain background (Reed et al., 1999), we were unable to construct a viable *pMET3::UBI4::DHFR^{ts}::3xHA::ABF1* degron allele in our S288C background despite several attempts and strategies. We, however, successfully created a *pMET3::UBI4::abf1(M1R)* allele in a strain carrying a *pGAL1::UBR1* allele. As described above, the ubiquitin moiety of the translated protein is cleaved off soon after translation, leaving an Abf1 protein capped with a destabilizing N-terminal arginine. Under inducing conditions, this Abf1-degron yielded growth arrest and displayed Abf1 depletion (Figures 1C and
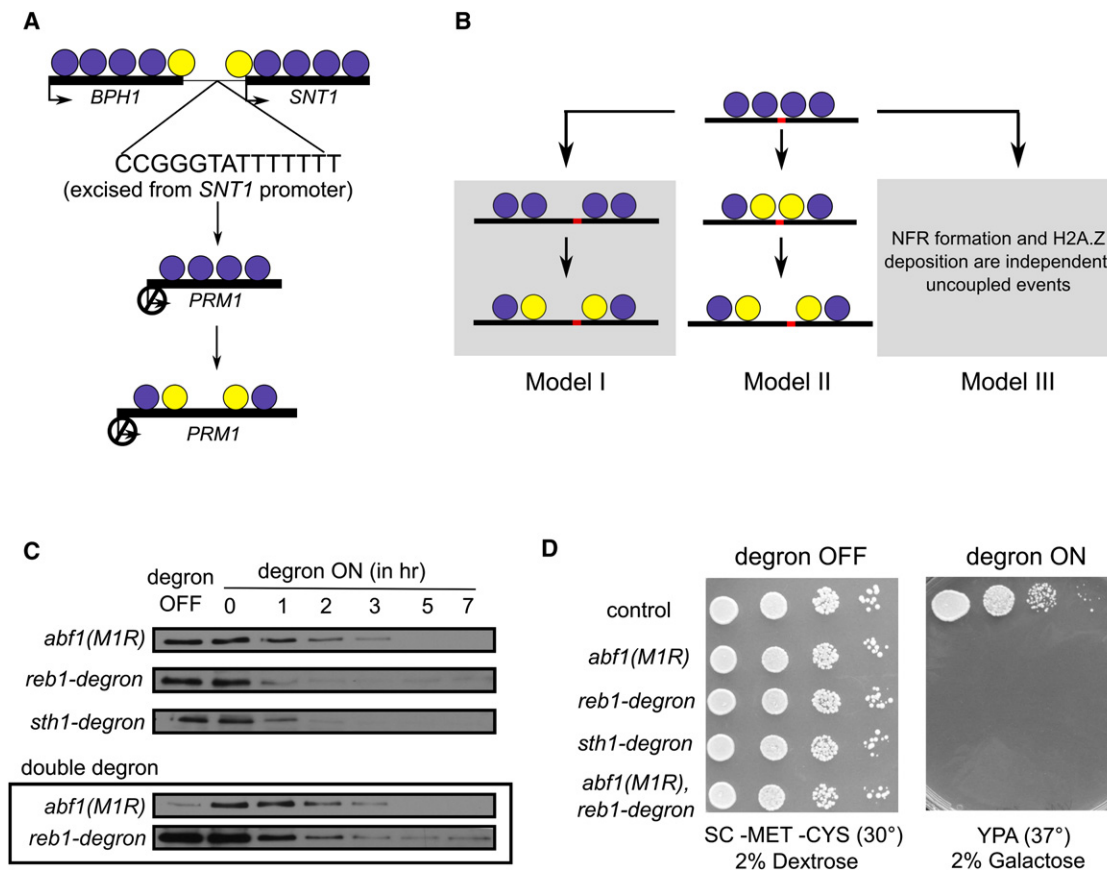
Figure 1. Models and Tools

(A) Diagram of the Reb1:dT$_7$ signal used in this study. Circles indicate nucleosomes. Yellow circle indicates H2A.Z variant nucleosome.

(B) Models for relationships between NFR formation and H2A.Z deposition.

(C) Conditional degron alleles of *ABF1, REB1* and *STH1* display protein depletion under degron-inducing conditions. Strains were shifted to YPA media containing 2% galactose for the indicated times and analyzed by immunoblotting with anti-HA or anti-Abf1 antibodies. Ponceau staining of blots demonstrated equal protein loading (Figure S1).

(D) Growth of degron strains under noninducing and inducing conditions. Shown are serial dilutions of strains plated on the indicated media. Plates were photographed after 2 days of incubation.

1D). We also constructed an Abf1 Reb1 "double degron" strain in order to simultaneously deplete both factors from cells (Figures 1C and 1D). For the studies described below, we determined nucleosome positions by hybridizing mononucleosomal versus genomic DNA-derived probe with in-house printed custom tiling arrays that span *S.cerevisiae* chromosome III at 20bp resolution (Yuan et al., 2005). The arrays also included oligonucleotides that tiled sequences corresponding to the *PRM1* gene to allow us to observe nucleosome positions programmed by Reb1:dT$_7$ (see Experimental Procedures for details). Unless otherwise specified, all experiments represent averages of four independent, biological replicates.

NFR Formation Mediated by a Reb1-Binding Site Requires Reb1 and the Chromatin Remodeling Complex RSC, but Not H2A.Z

As expected from our previous study (Raisner et al., 2005), nucleosome position analysis of the *PRM1* ORF with or without a Reb1:dT$_7$ insertion revealed that the insertion produces an NFR (Figure 2A). NFR formation was unaffected in strains carrying the Reb1-degron or Sth1-degron alleles under conditions in which the degron system was inactive (Figure 2B). We mapped nucleosome positions in strains carrying the Reb1-degron or the Sth1-degron five hours after activating the degron system, and these positions were compared to nucleosome positioning data from a control strain isogenic to the degron strains except that it lacked the Reb1 or Sth1 degron allele. The latter control strain was subjected to the identical culture growth protocol as the experimental strains. Depletion of Reb1 resulted in loss of the NFR programmed by Reb1:dT$_7$ inserted into the *PRM1* ORF, consistent with a direct role for Reb1 (Figure 2B). Likewise, inactivation of the RSC complex through depletion of Sth1 resulted in complete loss of the NFR programmed by the Reb1:dT$_7$ sequence (Figure 2B), supporting the hypothesis that Reb1 functions by recruiting RSC.

Model II above proposes that NFR formation requires the prior deposition of H2A.Z into chromatin, which is mediated by the

A
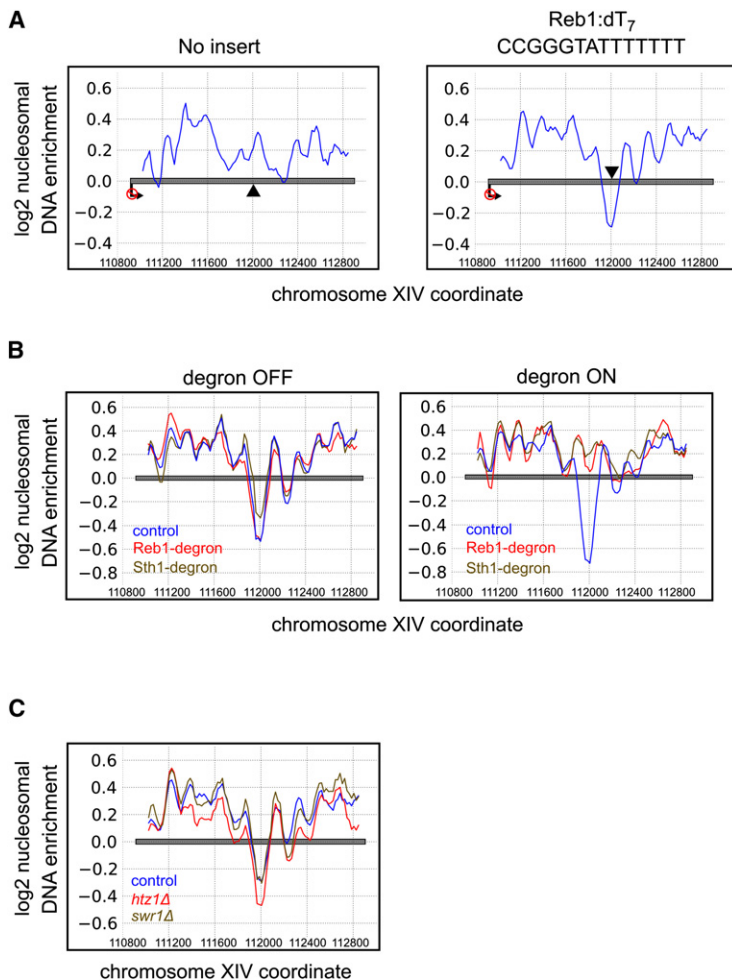
Figure 2. Tiling Array Analysis of Nucleosome Positions in the *PRM1* ORF Containing the Reb1:dT$_7$ Insertion

(A) Analysis of the effect of Reb1:dT$_7$ sequence insertion on nucleosome positioning. Shown are line traces of a moving average of mononucleosome/genomic probe signals across the *PRM1* gene with and without the indicated sequence insertion. Triangles indicate the insertion site.

(B) Analysis of effects of Reb1 and Sth1 depletion on NFR formation mediated by Reb1:dT$_7$. Indicated strains containing the Reb1:dT$_7$ insertion in the *PRM1* gene were analyzed as described in (A).

(C) Analysis of effects of *htz1Δ* and *swr1Δ* mutations on NFR formation mediated by Reb1:dT$_7$. Indicated strains containing the Reb1:dT$_7$ insertion in the *PRM1* gene were analyzed as described in (A).

Reb1 Is Required for the Formation of a Subset of NFRs

We next examined the chromosome-wide requirement for Reb1 in NFR formation. We mapped and compared nucleosome positions in the Reb1-degron strain and an isogenic control strain that lacked the Reb1-degron under conditions described above. Figure 3A shows a gene-by-gene "difference map" of the positioning data in which genes were aligned to each other based on the position of the +1 nucleosome downstream of the NFR in control strains and then the control signal subtracted from the mutant signal (yellow indicates more nucleosomal DNA signal in the mutant than in wild-type cells). The data were organized by K-means clustering. Two clusters are evident, one in which positioning was affected (Cluster I affecting 12% of assayed promoters), and another where no effect was evident (Cluster II). Line traces of the average signals of the control and degron strains for these two clusters are shown in Figure 3B. Inspection of Cluster I indicates that the two NFR-flanking nucleosomes move inward toward the center of the NFR, and this movement propagates further such that other flanking nucleosomes also shift their positions (Figure 3B). Figure 3C shows that the changes in the size of the trough signal representing the NFR between degron and control strains were dependent on the induction of the degron.

A previous study of transcription factor association at promoters assigned likelihood scores for a given transcription factor binding to a given promoter (Harbison et al., 2004). We compared these scores for Reb1 to the highest fold-change probe in the NFRs of promoters we assayed that were assigned scores. As shown in Figure 3D, there was a significant correlation (p = 7.81×10^{-7} based on a hypergeometric test using a likelihood score cutoff of p < 0.05). Consistent with this finding, promoters that contained at least one copy of the most conserved Reb1-binding site (TTACCCG [Liaw and Brandl, 1994]) tended to experience changes in NFR structure (Figure 3E). Cluster I was enriched for the most conserved Reb1 consensus site; indeed, 14 out of the 18 promoters in Cluster I contained this motif (p = 5.07×10^{-13}, Figure 3F). Relaxing the consensus to reflect the poorer conservation of the first two residues of the consensus still yielded highly significant enrichments (Figure 3F).

Swr1 chromatin remodeling complex. We tested whether H2A.Z or Swr1 is required for NFR formation induced by the Reb1:dT$_7$ signal. We constructed *htz1Δ* and *swr1Δ* strains and mapped the nucleosome positions in these strains. NFR formation mediated by insertion of Reb1:dT$_7$ at *PRM1* did not require H2A.Z or Swr1 (Figure 2C).

To test whether NFR formation at *PRM1* might be a consequence of transcription, we examined whether NFR formation induced by Reb1:dT$_7$ was associated with the production of transcripts. Transcript levels were examined using RT-PCR analysis of extracted total RNA. In a control strain in which the *PRM1* gene was induced with mating pheromone for 1hr, a specific signal was obtained (see Figure S2 available with this article online). We examined strains containing the insert and the Sth1 degron under both degron-inducing and permissive conditions as well as a strain lacking the insert. In these three cases, multiple peaks rather than a single peak were obtained in the QPCR melting curves indicating that cross-reacting cDNAs, instead of products specific to the *PRM1* locus, were being detected. Moreover, no quantitative differences were observed (Figure S2). Taken together, these data suggest that NFR formation was not associated with transcription that could be detected by these methods.
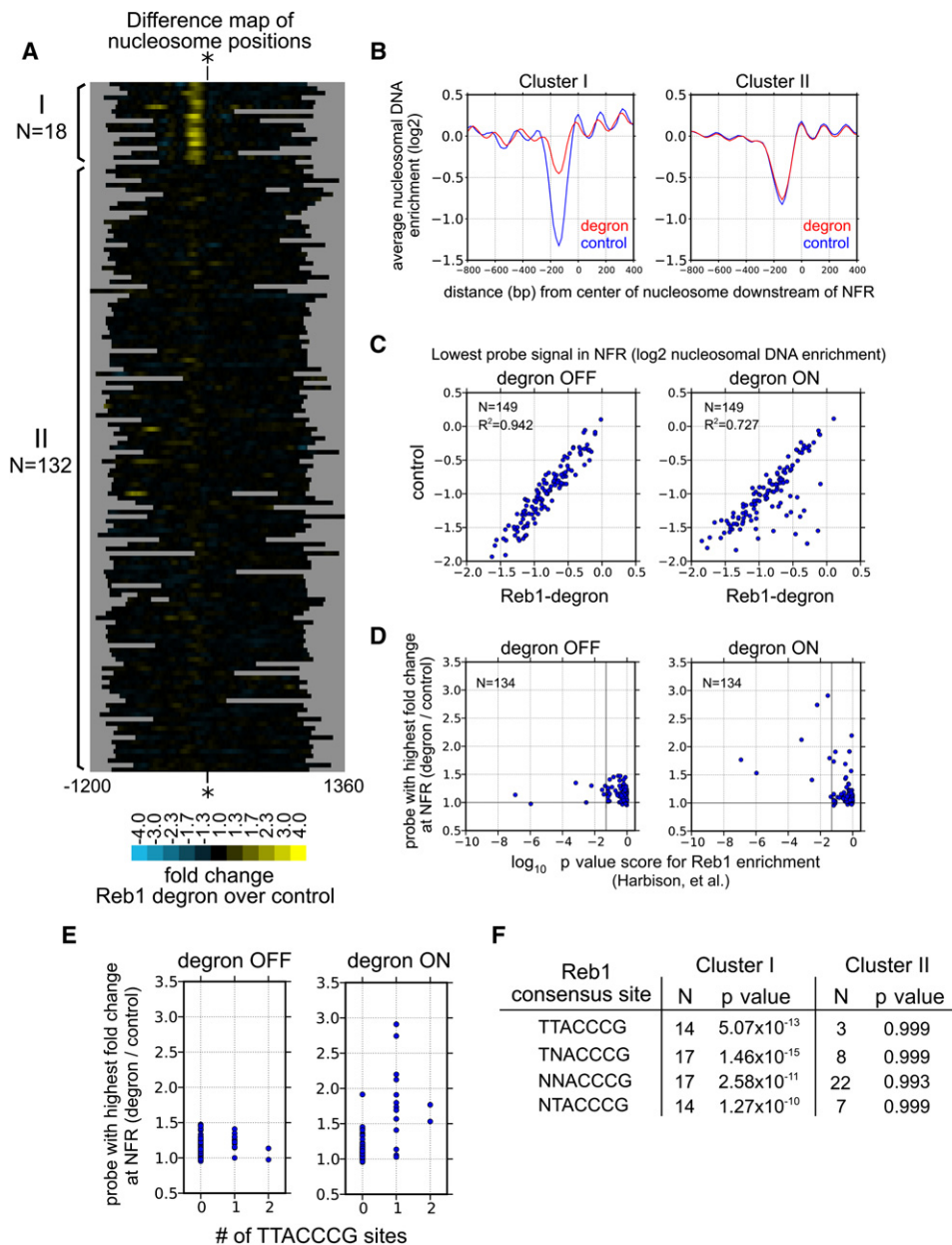
Figure 3. Chromosome-Wide Tiling Array Analysis of Nucleosome Positions in Cells Depleted of Reb1

(A) Difference map analysis of effects of Reb1 depletion on nucleosome positions. Map represents nucleosome positioning data from a control strain lacking the Reb1-degron subtracted from a strain with the Reb1-degron. See Experimental Procedures for further details. Nucleosome positioning data 1kb upstream and downstream of the ATG of 150 genes are shown and orientated such that the direction of transcription is to the right. Asterisks indicate center of the +1 nucleosome downstream of the NFR in the control strain. The x axis represents the distance (in bp) from the center. Data are organized into two clusters using the k-means method.

(B) Line traces of average nucleosome positions of the two clusters shown in (A). The indicated strains were grown under degron-inducing conditions.

(C) Scatter plots of the lowest probe signal in NFRs. Points indicate the lowest probe signal in the NFR for a locus in control versus degron strains grown under the indicated conditions.

(D) Correlation between Reb1 binding and changes in nucleosomal enrichment at NFRs at promoters. The significance values (log10 p-value) of Reb1 binding at promoters (Harbison et al., 2004) are compared against the highest fold changes of nucleosome positioning signals at the associated NFR.

(E) Correlation between Reb1 consensus sites in promoters and the highest fold change of nucleosome enrichment at the associated NFR under the indicated promoters.

(F) Enrichment of Reb1 sites in clusters. Shown are the p-values (hypergeometric testing) of the significance of the indicated Reb1 motifs in the indicated clusters.
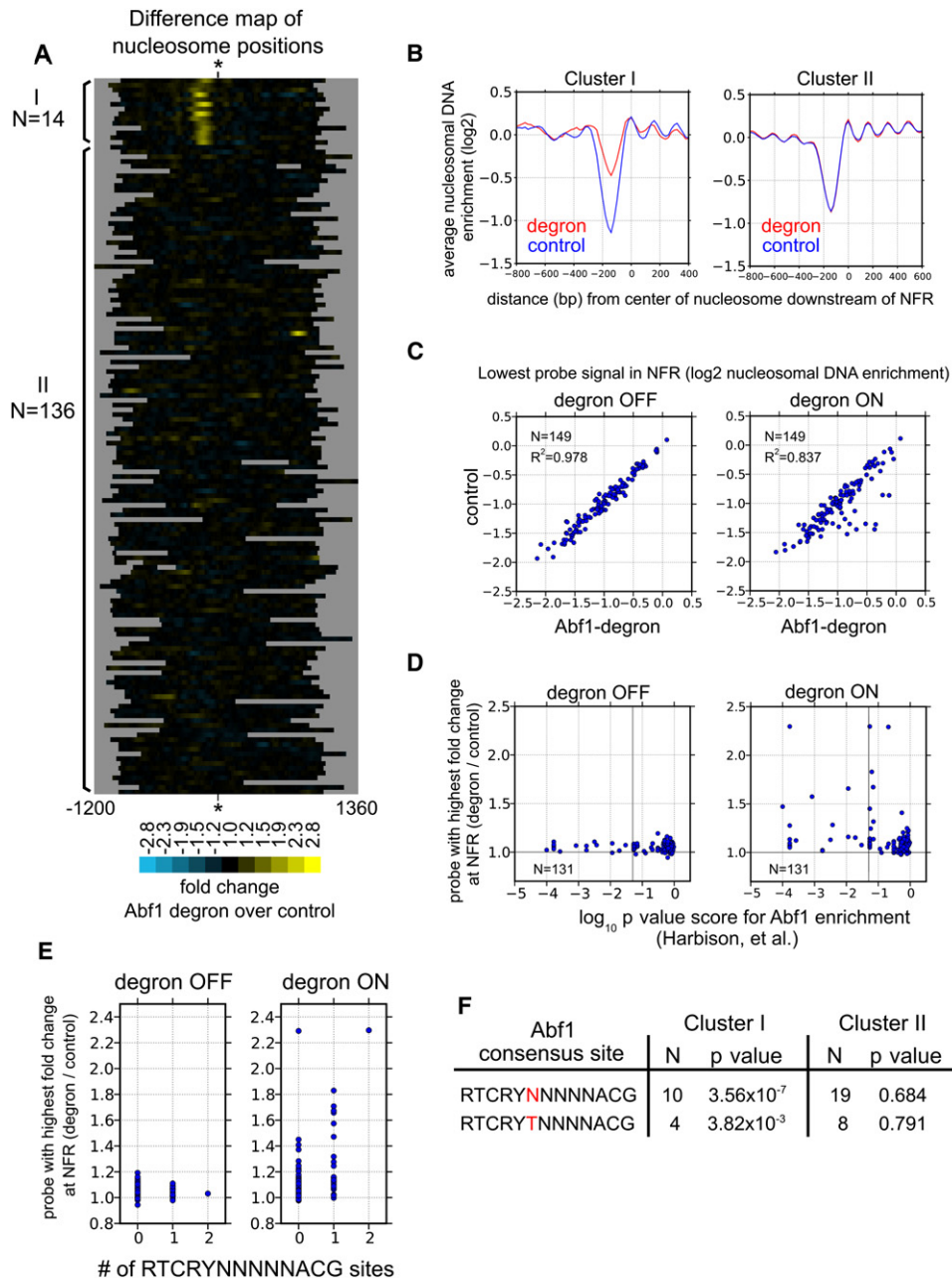
Figure 4. Chromosome-Wide Tiling Array Analysis of Nucleosome Positions in Cells Depleted of Abf1

(A–F) These panels are analogous to those of Figure 3 except that a strain with the Abf1-degron was compared to the same control strain used for analysis of nucleosome positions upon Reb1 depletion.

Abf1 Is Required for the Formation of a Subset of NFRs

We next performed the same analysis on the Abf1 degron strain. Difference map analysis and clustering (Figure 4A) show that 9.3% of promoters were affected, and these promoters were distinct from promoters affected by Reb1 depletion (see below). As with the Reb1 degron, the affected cluster displays a smaller NFR and movement of flanking nucleosomes toward the NFR (Figure 4B), and these changes were dependent on induction of the degron (Figure 4C). Likewise, affected NFRs were

enriched for Abf1 binding (Figure 4D) and for an Abf1 consensus site (Figures 4E and 4F). The latter correlations are weaker than for the Reb1 site, perhaps because of the higher degeneracy of the Abf1 consensus site (Beinoraviciute-Kellner et al., 2005).

RSC Is Required for Proper Positioning of NFR-Flanking Nucleosomes

We next examined the effects of Sth1 depletion on nucleosome positioning using strains carrying the Sth1-degron as described
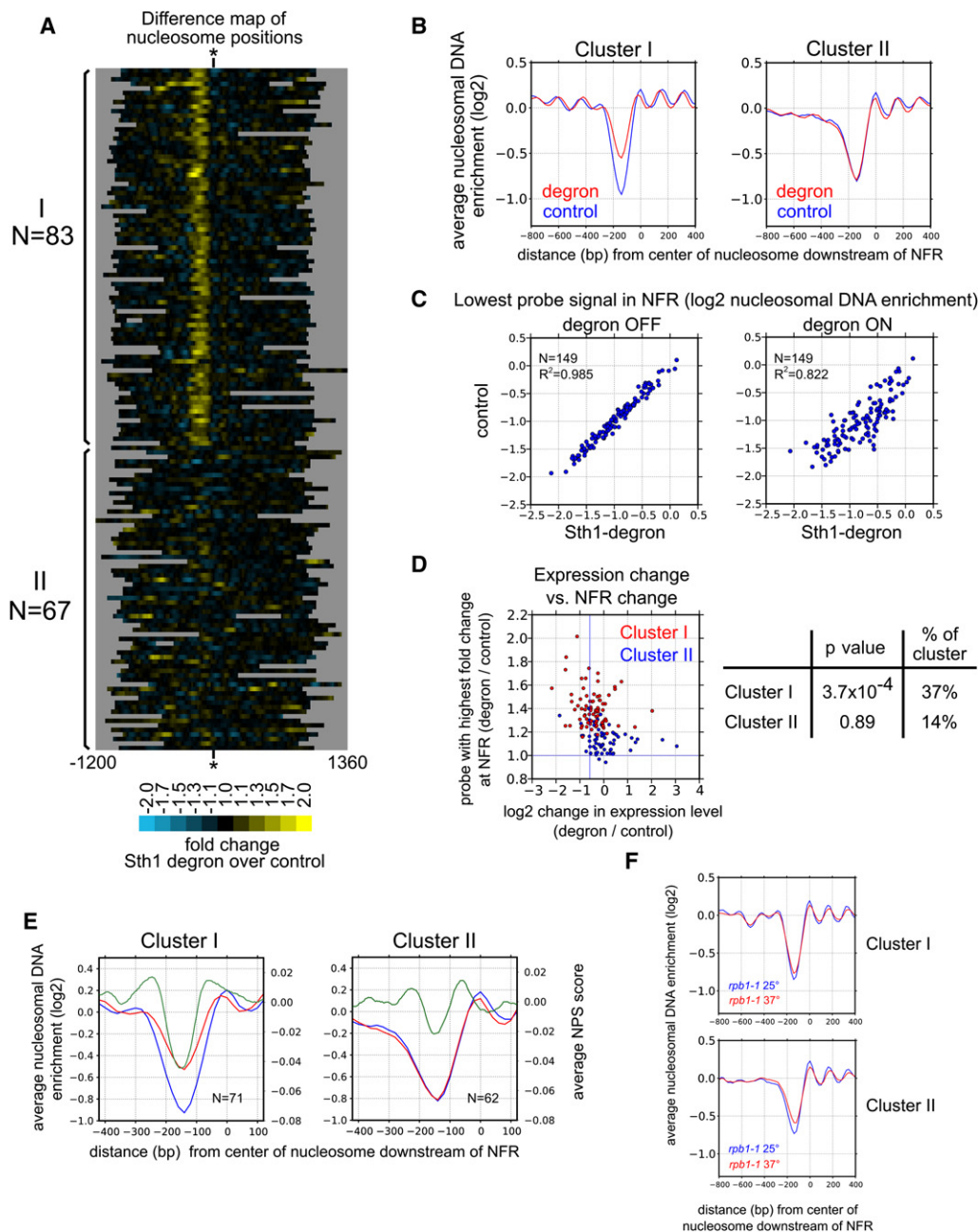
Figure 5. Chromosome-Wide Tiling Array Analysis of Nucleosome Positions in Cells Depleted of Sth1

(A–C) These panels are analogous to those of Figure 3 except that a strain with the Sth1-degron was compared to the same control strain used for analysis of nucleosome positions upon Reb1 depletion.

(D) Gene expression analysis. Shown is the correlation between mRNA and NFR changes in cells depleted of Sth1. Ploted are the values for genes on chromosome III. Shown on right is the p-values (hypergeometric testing) of the significance of the enrichments in the indicated gene groups using a 1.5-fold cutoff for decreases in mRNA levels. Expression data were not available for all genes in the clusters; hence, Cluster I n = 79, Cluster II n = 64.

(E) NPS signature averages. Lines traces of NPS predictions (Ioshikhes et al., 2006) for genes in the indicated gene clusters are shown in green. These predictions were smoothed using a 51bp moving average window. Experimental nucleosome position averages (control is blue, Sth1-degron is red) are shown as in panel (B).

(F) Effect of transcription on nucleosome positioning. Shown are the average nucleosome positions for the indicated gene clusters in *rpb1-1* strains grown under permissive conditions or for 1 hr under nonpermissive conditions.

above. Strikingly, our analysis showed that Sth1 depletion affected a majority (55%) of promoters (see Cluster I in Figure 5A). The affected cluster displayed shrinking of the NFR and movement of flanking nucleosomes, whereas little change in nucleosome position was apparent for members of Cluster II (Figure 5B). As with the Reb1 and Abf1 degron strains, growth

under degron-inducing conditions was required to observe these differences (Figure 5C). Figure S10B shows a superposition of a histogram of the locations of mapped TSSs (Nagalashmi et al., 2008) and the positioning data. Consistent with previous studies, TSSs tend to lie just inside the downstream nucleosome and the movement observed in Sth1-depleted cells moves these sites further into the nucleosome core (Figure S3). This may explain why RSC depletion has been reported to cause cessation of transcription by RNA polymerase II (Parnell et al., 2008).

When RSC, Abf1, or Reb1 were depleted, NFRs shrank but were not eliminated. We hypothesized that intrinsic positioning sequences might explain the positions of nucleosomes under these conditions. Therefore, we compared the positions we observed in Cluster I of Sth1-depleted cells with those predicted by Pugh and colleagues (Ioshikhes et al., 2006) based on AA/TT dinucleotide periodicity enrichment. As shown in Figure 5E, the average nucleosome position of the +1 and −1 nucleosomes of Cluster I relax toward positions specified by the NPS signature. For the largely unaffected cluster (Cluster II), a discrepancy between the NPS-predicted and observed positions is still apparent for the +1 nucleosome, whereas the −1 nucleosome is poorly aligned in this despite the sharp NPS prediction peak (Figure 5E).

To test whether Sth1 depletion results in changes in gene expression, we performed expression profiling of the Sth1 degron strain against a control strain under degron-inducing conditions. As we expected global changes in gene expression, we incorporated external spiked-in RNA controls into our normalization procedure (see Experimental Procedures). We then asked whether there was an enrichment for genes whose expression was reduced in Sth1-depleted cells in Cluster I versus Cluster II. As shown in Figure 5D, Cluster I is indeed highly enriched for genes whose expression requires Sth1, indicating that that the changes in positioning correlate with changes in expression. Given this result, we tested whether loss of transcription might be responsible for changes in positioning. We mapped nucleosome positions in a temperature-sensitive RNA polymerase II strain (*rpb1-1*) which ceases transcription within minutes upon shift into restrictive conditions (Nonet et al., 1987). The *rpb1-1* mutant was grown at either 25°C or shifted for 1 hr to 37°C. The average nucleosome positions in these conditions were determined for Clusters I and II of the Sth1 degron difference map. There were were no detectable differences in nucleosome positions in either cluster (Figures 5F and S4). Hence, the changes in NFR structure observed upon Sth1 depletion appear to be due to the action of RSC rather than from cessation of transcription per se.

Abf1 and Reb1 Are Required for NFR Formation at Distinct Sets of Promoters

To identify promoters that are redundantly controlled by Abf1 and Reb1, we examined a double degron strain that carried the Abf1-degron and Reb1-degron alleles (Figures 1C and 1D). The resulting difference map was clustered together with difference maps for the Abf1 single degron strain, the Reb1 single degron strain, and the Sth1 degron strain (Figure 6A; Figure 6B shows that NFR changes in the double degron are dependent

on degron induction). K-means clustering revealed that the promoter NFRs affected by loss of either Abf1 or Reb1 were reproducibly affected in the double degron strain, but there were no other promoter NFRs that were significantly affected in the double degron strain. It is also evident that most NFRs affected by loss of Reb1 also required Sth1 for proper positioning of nucleosomes (Figure 6A), consistent with the data obtained with the synthetic NFR described above (Figure 2B). The NFRs affected by loss of Abf1 appeared to have a somewhat lesser degree of dependence for Sth1 for nucleosome positioning (Figure 6A). Likewise, there clearly are many NFRs that require RSC, but not Abf1 or Reb1, for proper nucleosome positioning (Figure 6A), suggesting the existence of additional RSC recruitment mechanisms. Analysis of average nucleosome positions for each cluster indicates that the the changes observed (Figure 6A) are due to shifts in nucleosome positions (Figure S5).

As with the Sth1 degron strain, we examined the Abf1- Reb1- double-degron strain for changes in transcript levels using whole genome microarrays and spiked-in external controls. As shown in Figure 6C, we found a significant correlation between decreases in NFR size and decreases in transcript accumulation.

## H2A.Z Deposition Is Generally Dispensable for Nucleosome Positioning

To complete our analysis of positioning, we used cells lacking H2A.Z (*htz1Δ*) or lacking the ATPase subunit of its deposition complex (*swr1Δ*) to determine whether H2A.Z exchange was required for nucleosome positioning chromosome-wide (Figure S6). Based on the results with the synthetic NFR (Figure 2C), we expected to see no differences in positioning. Indeed, as shown by line traces of the average positions of aligned promoter nucleosomes, H2A.Z deposition resulted in no detectable changes. Of course, we cannot rule out the possibility that there could be changes too subtle to observe using our 20bp resolution tiling arrays.

Development an Inducible H2A.Z Deposition System

Nonetheless, these data argue against Model II (Figure 1B), which proposed that H2A.Z deposition is essential for NFR formation. We then considered the two remaining models: (1) the deposition of H2A.Z at a promoter requires the presence of an NFR at that promoter (Model II), or (2) H2A.Z deposition occurs independently of NFR formation (Model III). In principle, these models could be distinguished through development of a system in which NFR loss is induced under conditions where H2A.Z is not deposited into chromatin, but then H2A.Z is induced and its deposition examined. The Sth1 degron provides a tool to trigger abrogation of the synthetic NFR programmed by Reb1:dT$_7$ and shrinkage of bona fide promoter NFRs. However, since global transcription is shut off in RSC-depleted cells, we sought a posttranslational method to control H2A.Z deposition.

We utilized an engineered *M. tuberculosis* RecA intein whose intrinsic protein splicing is controlled by the human estrogen receptor ligand-binding domain (Buskirk et al., 2004). This construct was used previously to interrupt several coding sequences in yeast, and its splicing was shown to be activated
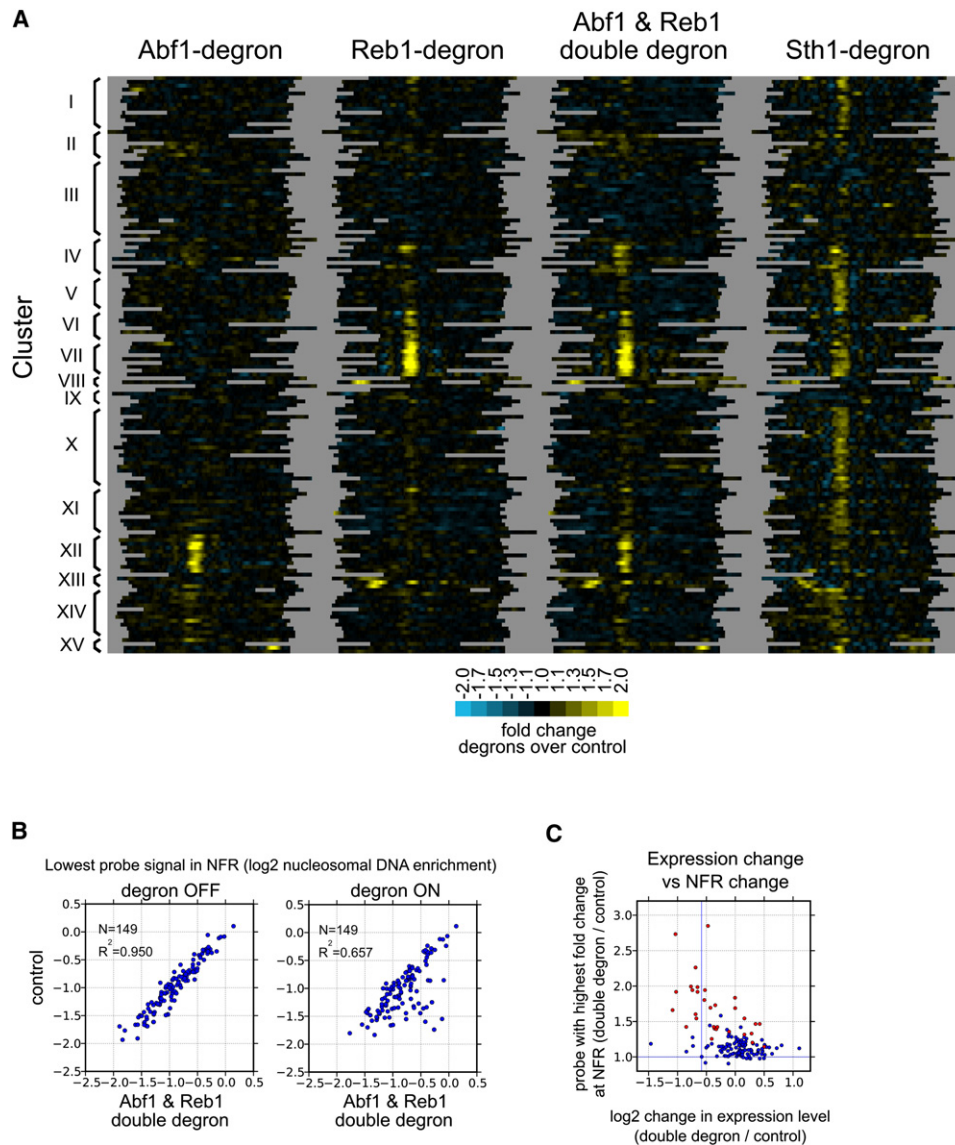
Figure 6. Comparison of the Roles of Abf1, Reb1, and RSC in Nucleosome Positioning

(A) Clustering analysis of difference maps. Shown are difference maps for the indicated strains including the Abf1-Reb1 "double degron" strain. K-means (K = 15) clustering was applied. Line traces of cluster averages are shown in Figure S14.

(B) Scatter plots of double degron. Analysis was performed as in Figure 3C.

(C) Gene expression analysis. Shown is the correlation between mRNA and NFR changes in cells depleted of both Reb1 and Abf1. The p-value (hypergeometric testing) of the significance of the enrichments in the group of genes (n = 20) consisting of those affected in NFR size by Abf1- or Reb1-depletion (Cluster I in Figure 3 and Cluster I in Figure 4; corresponding points are colored red in this figure) using a 1.5-fold cutoff for decreases in mRNA levels was 1.2×10^{-6}. The p value for the remaining, unaffected genes (n = 123) was 0.99.

in vivo using the estrogen agonist 4-hydroxytamoxifen (4-HT). The chemistry of splicing requires cysteine cleavage sites and leaves a single cysteine residue at the splice junction.

We initially targeted the Swr1 and Swc2 subunits of the Swr1 complex by inserting the intein construct before the codons for several native cysteine residues in the corresponding genes. These alleles abrogated H2A.Z deposition in *vivo*, but addition of 4-HT did not restore H2A.Z deposition (unpublished observations), suggesting that the placement of the intein was incompat-

ible with protein stability and/or intein splicing. We next attempted engineering a spliceable *HTZ1* allele under the assumption that the smaller size of H2A.Z relative to the intein construct would make the protein context less likely to interfere in proper structural formation of the intein. H2A.Z, however, lacks cysteine residues, so such a spliced allele would by necessity contain a cysteine point mutation. Four H2A.Z residues (Ala46, Thr68, Thr88 and Asp100) that did not confer a significant growth defect in high precision measurements when mutated (S. Braun,
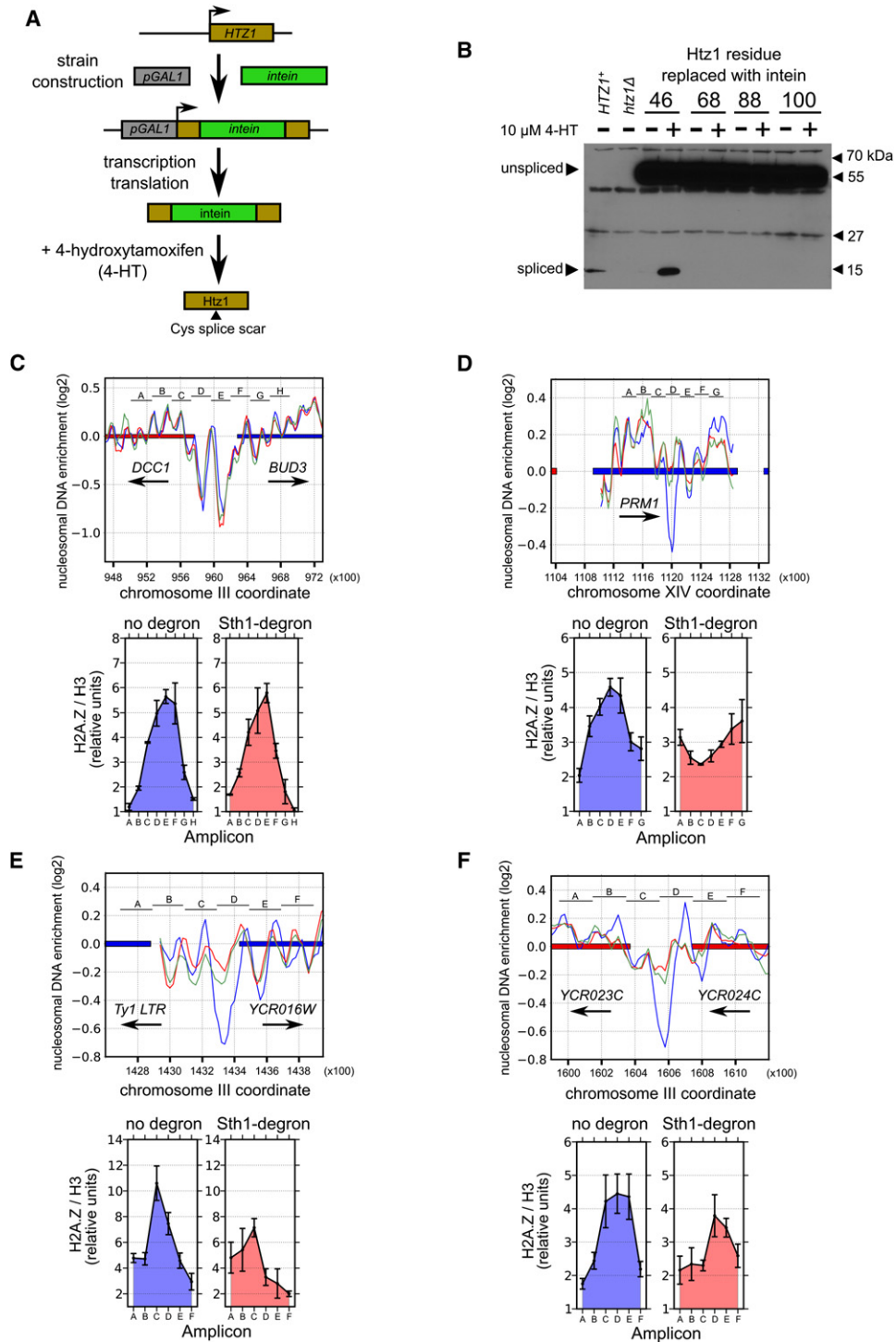
Figure 7. Analysis of H2A.Z Deposition Requirements Using a Steroid-Regulated Intein

(A) Schematic of H2A.Z intein constructs. An engineered *M. tuberculosis* RecA intein controlled by the human estrogen receptor ligand-binding domain was placed at a chosen site in *HTZ1* gene (encoding H2A.Z). The *HTZ1* promoter was replaced with the galactose-inducible *pGAL1* promoter. Protein splicing would occur in the presence of 4-hydroxytamoxifen (4-HT) and leave a cysteine residue ("scar") at the splicing junction.

(B) Splicing of the H2A.Z intein construct occurs with an allele that replaces Ala46 with the intein construct. The 4-HT-regulated intein was inserted in place of four different residues in H2A.Z, and these constructs each were placed on a 2 μ plasmid under the control of a *pGAL1* promoter and transformed into a *htz1Δ* strain. Strains were grown to mid-log phase in the presence of 2% galactose and, when indicated, 10 μM 4-HT. Shown is a western using polyclonal antibody specific to the C terminus of H2A.Z. A strain with a chromosomal-based, wild-type copy of *HTZ1* and a *htz1Δ* strain are included as controls.

D. Breslow, J. Weissman, and H.D.M., unpublished data) were replaced with the intein construct. These alleles initially replaced wild-type *HTZ1* at its native chromosomal locus, but none displayed detectable spliced product in the presence of 4-HT (unpublished data). We therefore placed these alleles under the control of a *pGAL1* promoter on a high-copy 2 micron plasmid vector. The allele in which Ala46 was replaced with the intein construct yielded a protein that was spliced in vivo when cultures were treated with 4-HT; Ala46 is a residue in the core histone fold domain (Figures 7A and 7B). As splicing produced somewhat higher levels of H2A.Z than in that found in wild-type cells (Figure 7B), we placed the construct on a low-copy *CEN-ARS* plasmid. Regulated splicing of the H2A.Z intein was also observed (Figure S7A), and this construct was used in further experiments. We refer to this *pGAL1::htz1(A46intein)* allele on a *CEN-ARS* plasmid as the H2A.Z intein construct.

We examined the deposition of H2A.Z whose synthesis was directed by this construct using chromatin immunoprecipitation (ChIP). Although splicing in the H2A.Z intein is regulated, a small amount of H2A.Z deposition was observed in the absence of 4-HT, presumably due to low levels of background splicing (Figure S7C); however, the H2A.Z enrichment signal steadily increases over time in response to 4-HT treatment (Figure S7D), indicating stimulation of H2A.Z deposition by the activation of splicing.

Focused H2A.Z Deposition in Response to Reb1:dT$_7$ Requires Prior NFR Formation by RSC

We introduced the H2A.Z intein into *htz1Δ* strains that carried *pGAL1::UBR1* and either the Sth1-degron or a wild-type Sth1. Simultaneous activation of the degron system and synthesis of unspliced H2A.Z were accomplished by transferring cells to 37°C media containing galactose. After 5 hr of growth, intein splicing was initiated by the addition of 4-HT, and cells were collected after 3 hr of further incubation at 37°C to allow for H2A.Z deposition. Chromatin immunoprecipitation for H2A.Z and histone H3 were carried out, and quantitative PCR was used to measure H2A.Z enrichment relative to H3 enrichment. The H2A.Z/H3 enrichment values were normalized to an amplicon in the middle of the large *BUD3* ORF where there is little detectable H2A.Z (Raisner et al., 2005). Nucleosome positions were also mapped for the Sth1-degron H2A.Z intein strain prior to degradation of Sth1, after 5 hr of Sth1 depletion, and 3 hr after addition of 4-HT. We determined that unspliced H2A.Z was being produced and was spliceable, and we found that Sth1 degradation still occurred in the presence of the H2A.Z intein construct and during 4-HT treatment (Figures S7A and S7B).

We sought to examine the deposition profiles of H2A.Z at NFRs whose structure is unaffected upon Sth1 depletion and at NFRs that undergo significant changes upon Sth1 depletion. The two NFRs located within an intergenic region containing the *DCC1* and *BUD3* promoters do not appear to require Sth1 for their organization (Figure 7C, top panel). The H2A.Z deposition profiles across the *DCC1-BUD3* intergenic region in both the Sth1-degron and control strains were similar (Figure 7C bottom) and indicated that H2A.Z deposition could still occur under these conditions. We next examined how loss of the NFR programmed by insertion of Reb1:dT$_7$ into *PRM1* affected the recruitment of H2A.Z. This NFR essentially collapses upon Sth1 depletion in the H2A.Z intein strain carrying the Sth1-degron (Figure 7D, top panel). In the strain that did not have the Sth1-degron and therefore maintained the NFR programmed by Reb1: dT$_7$ inserted into *PRM1*, H2A.Z deposition occurred in the middle of *PRM1*, with its peak deposition at the Reb1: dT$_7$ insertion site (Figure 7D, bottom left panel). In contrast, upon Sth1 depletion, there was no H2A.Z deposition focus about the Reb1: dT$_7$ insertion site (Figure 7D, bottom right panel). The apparently undirected, background H2A.Z deposition in the *PRM1* ORF is similar to that observed in cells lacking the Reb1:dT$_7$ insertion (Raisner et al., 2005), and similar global patterns of untargeted H2A.Z deposition have been seen in genome-wide studies (Albert et al., 2007). Thus, the focused peak of H2A.Z deposition induced by the Reb1:dT$_7$ DNA signal appears to require the Sth1-dependent formation of an NFR directed by the signal.

RSC depletion did not produce complete collapse of NFRs on endogenous promoters, and, as described above, this may be due to intrinsic positioning signals. Nonetheless, we examined the H2A.Z deposition profile at the promoters of *YCR016W* and *YCR023C*, both of which experience significant nucleosome encroachment into their NFRs upon Sth1 depletion (Figures 7E and 7F, top panels). We observed H2A.Z deposition at these promoters under conditions in which their NFRs were unaffected as well as under conditions where their NFRs were affected (Figures 7E and 7F, bottom panels). However, the H2A.Z deposition profile at affected NFRs differed in that there was a significant decrease in H2A.Z enrichment in the vicinity of the +1 nucleosome relative to the NFR (see amplicon "D" for Figure 7E and amplicon "C" for Figure 7F). Whether the otherwise fairly robust H2A.Z deposition seen at these two promoters under conditions of intein induction is explained by the presence of a residual NFR driven by NPSs or by NFR-independent mechanisms that stimulate H2A.Z deposition such as histone acetylation and its subsequent recognition by Bdf1 (Raisner et al., 2005) is not clear. The latter model is difficult to test since cells lacking H2A.Z and Bdf1 are inviable (Raisner et al., 2005).

DISCUSSION

Based on the results of a number of genome-scale studies, it has become increasingly clear in organisms as diverse as yeast and

---

(C–F) Analysis of H2A.Z deposition requirements. A strain carrying the Sth1 degron was shifted to degron-inducing conditions which also induces synthesis of unspliced H2A.Z intein construct. After 5 hr, 4-HT was added to 10 μM to induce splicing. Cells were collected after 3 hr of further incubation, and H2A.Z enrichment at select loci was determined relative to histone H3 enrichment and normalized to a locus in the middle of the large *BUD3* ORF. H2A.Z/H3 enrichment profiles under Sth1-depleted conditions were compared against control profiles. The promoters of *DCC1/BUD3* are analyzed in (C); the *PRM*1 ORF containing the Reb1:dT$_7$ insertion is analyzed in (D); the promoter of *YCR016W* is analyzed in (E), and the promoter of *YCRO23C* is analyzed in (F). Top panels of (C–F) indicate nucleosomal DNA enrichment in various conditions (blue: degron-OFF conditions, red: 5 hr of degron-ON, green: 8 hr of degron-ON, with the last 3 hr in the presence of 4-HT). Bottom panels of (C)–(F) represent normalized H2A.Z/H3 enrichment values at the indicated amplicons, and the error bars represent the S.E.M.

humans that gene regulatory regions display stereotypical patterns of nucleosome positioning and identity. Although there are species-specific differences, promoters are generally characterized by an NFR flanked by at least one H2A.Z nucleosome. Despite the power of these descriptive genome-wide studies as well as work that indicates that these characteristics of promoters play key roles in gene regulation (see Introduction for references), they leave open the question of how these structures are programmed.

Two lines of studies have come to distinct conclusions regarding NFR formation mechanisms. One group of studies has suggested that the direct effects of sequence on DNA-octamer affinity programs NFR formation (see Introduction for references). In contrast, our previous work defined a short signal from the *SNT1* gene containing a putative site for a DNA-binding protein, Reb1, that is sufficient to program a NFR flanked by H2A.Z nucleosomes when placed into the middle of a positioned nucleosome in an inactive gene (Raisner et al., 2005). Others have also implicated Reb1 and Abf1 in the formation of nucleosome gaps within the specific promoter regions (Angermayr et al., 2003; De Winde et al., 1993). The work described here helps reconcile these two lines of research and provides insight into the relationship between NFRs and H2A.Z deposition. Our principal conclusions are as follows.

RSC Displaces NFR-Flanking Nucleosomes Away from Their Average NPS-Predicted Positions

A striking result presented here is that at a majority of promoters, the normal positioning of NFR-flanking nucleosomes requires the essential multisubunit chromatin modeling complex RSC. Such a central role for RSC in generating promoter chromatin architecture is consistent with several of its properties: (1) RSC, unlike most chromatin remodeling enzymes in yeast, is essential for viability (Cairns et al., 1996, 1999), (2) RSC slides nucleosomes in vitro (Lorch et al., 2001), and (3) RSC is required globally for RNA polymerase II transcription (Parnell et al., 2008). Our studies are also consistent with a recent lower-resolution study that concluded that RSC affected histone density at a number of promoters (Parnell et al., 2008). A recent study indicated changes in the positioning nucleosomes at ~12% of promoters in cells lacking the Isw2 chromatin remodeling complex (Whitehouse et al., 2007). The primary function of Isw2 appears to be in transcriptional repression and in suppressing antisense transcription (Whitehouse et al., 2007). Interestingly, in contrast to RSC, Isw2 appears to move nucleosomes in vivo toward the NFR, raising the possibility that it antagonizes the action of RSC at some promoters. The potential for dynamic involvement of multiple ATPases at promoters further underscores the active nature of mechanisms that position nucleosomes in vivo.

The finding in this study and in the previous study that the final resting positions of nucleosomes are strongly influenced by ATP-dependent chromatin remodeling mechanisms argues that that the intrinsic affinity of the octamer for underlying DNA sequences is not determinative for the final positioned state. However, our observation that depletion of Sth1 causes nucleosome positions to relax on average closer to those predicted by an NPS signature strongly suggests that sequence properties

play a role in a stepwise mechanism for NFR formation. That is, NPS-mediated positioning exposes binding sites for factors such as Reb1 and Abf1, which in turn induce the action of RSC to move nucleosomes to their steady-state average positions in wild-type cells. Such a model is also consistent with in vitro and in vivo observations that suggest that the Isw2 remodeling enzyme moves nucleosomes into energetically unfavorable sites (Whitehouse and Tsukiyama, 2006). We speculate that, compared to a purely "hard-wired" system, this more dynamic, ATP-dependent mechanism may facilitate binding of DNA-binding proteins to nucleosomal sites and transcription initiation. It is important to note that NPS predictions vary in their accuracy considerably at the level of individual genes, suggesting they likely do not predict with full accuracy the intrinsic thermodynamics of octamer-DNA interactions. A histogram of predictions (Ioshikhes et al., 2006) reveals that NPS-predicted positions for individual genes deviate significantly from experimental positions even in the Sth1 degron strain (Figure S8). Nonetheless, the close correspondence of the average profiles supports the two-step model proposed above.

Sequence-Specific DNA-Binding Proteins Are Required for Positioning of NFR-Flanking Nucleosomes at a Significant Fraction of Promoters

Using a signal for NFR formation/H2A.Z deposition we identified previously, we demonstrated a role for the Reb1 protein and RSC for NFR formation programmed by this isolated signal. Given the previously reported biochemical interactions between Reb1 and subunits of RSC, the simplest interpretation is that recruitment of RSC by Reb1 generates the NFR. Our examination of the generality of this mechanism across chromosome III suggests that a subset of promoters, enriched for Reb1-binding sites, use this mechanism in a nonredundant fashion. Abf1, another essential Myb family member, operates at a distinct subset of promoters. These observations are consistent with studies that show that Reb1 and Abf1 sites are highly enriched in NFRs compared to the binding sites for nearly all other studied DNA-binding proteins (Lee et al., 2007). The remaining promoters presumably target RSC and other remodeling mechanisms through other means. In this regard, it is interesting to note that four subunits of RSC contain potential DNA-binding domains. Using standard ChIP protocols as well as ones using additional crosslinking agents, we have been unable to detect either wild-type Sth1 or an induced catalytically-dead version of Sth1 at the Reb1:dT$_7$ signal inserted into *PRM1,* suggesting transient binding of RSC to this site (unpublished data). Likewise, only a fraction of intergenic regions display RSC binding in published ChIP-chip experiments (Ng et al., 2002), despite the global requirement for RSC in pol II transcription (Parnell et al., 2008). We suggest that at many sites of action the off-rate of the RSC complex in vivo may be too high to allow detection by ChIP.

H2A.Z Deposition Is Dispensable for NFR Formation but NFR Formation Promotes H2A.Z Deposition

We find no evidence that nucleosome positioning in general requires H2A.Z deposition. While a previous report suggested that H2A.Z controls nucleosome positioning in vivo, this conclusion was largely based on a single 20bp shift observed in the

position of a nucleosome in the *GAL1* promoter in *htz1Δ* cells (Guillemette et al., 2005). Another study examined nucleosome positioning in *htz1Δ* cells at four other loci (*SUC2*, *COQ3*, *POS5*, and *COQ1*), which are all highly enriched for H2A.Z and saw no differences in positioning (Li et al., 2005). Our results are generally in line with the latter study. However, we note that the technology used in our study, while cost-effective and allowing for multiple experimental replicates, does not have the ability to detect shifts of less than 20bp. Thus, we cannot rule out the possibility that our studies would have missed a more subtle role for H2A.Z deposition in nucleosome positioning.

To explore the relationship between NFR formation and H2A.Z deposition we implemented a steroid-regulated protein splicing strategy to induce H2A.Z deposition under conditions in which NFR structure was abrogated by depletion of Sth1 Our data show that deposition of H2A.Z about the NFR programmed by insertion of Reb1:dT$_7$ into *PRM1* required the prior action of Sth1, which presumably acts to induce formation of the NFR. This defect in deposition was not due to a general defect in H2A.Z deposition in RSC-depleted cells as normal deposition occurred at the *BUD3-DCC1* intergenic region and significant albeit reduced H2A.Z deposition occurred at the promoters of two genes whose NFRs shrank in response to RSC depletion. Our results predict that in vitro studies of the exchange activity of the purified Swr1 deposition complex may show a dependence on adjacent nonnucleosomal DNA. Such a property would not be without precedence as the ACF complex has been shown to have nucleosome-sliding catalytic activity that is stimulated in vitro by flanking DNA (Yang et al., 2006). These observations may explain the general linkage observed in yeast, plants and metazoans between NFRs of various sizes and enhanced deposition of H2A.Z in flanking nucleosomes.

EXPERIMENTAL PROCEDURES

Yeast Strains
The strains used in this study are described in Table S1. Yeast transformants were generated by conventional lithium acetate and polyethylene glycerol procedures with selectable or counter-selectable transforming DNA. Insertions at the *PRM1* ORF were obtained by a two-step process in which a construct containing I-SceI and its restriction site was first inserted and subsequently replaced with a desired sequence (Storici et al., 2003).

Gene Expression Profiling
For each strain, total RNA from four independently grown cultures was prepared using a TRIZOL procedure and spiked with RNA from the Agilent Dual-color RNA Spike-in Kit. Aminoallyl-dUTP-labeled probe was generated by reverse transcription, and hybridizations were carried out using 4x44k Agilent microarrays that cover 6256 *S. cerevisiae* features, each of which are replicated 7 times on the array (Agilent design ID 015072). Dye swaps were incorporated such that for each experiment, there were 2 arrays of one dye configuration, and vice-versa. Data normalization was performed using a composite loess procedure that used 1:1 DCP probes for the spike-in loess curve (Yang et al., 2002). Expression ratios for each gene per array then were derived by calculating the mean of up to 7 technical replicates, while discarding any replicates that were not within 2 standard deviations.

Mapping Nucleosome Positions Using Tiling Microarrays
Nucleosome positions were mapped by hybridizing probe representing mononucleosomal-sized DNA against genomic reference DNA. Mononucleosomal-sized probe was obtained from chromatin isolated from cultures that had been grown to an OD$_{600}$ of 0.7-0.9 prior to 1% formaldehyde crosslinking for 15 min at the same growth temperature and followed by a 0.125 M glycine quench. Genomic reference probe was obtained from purified genomic DNA. Detailed explanations of the microarray platform and how the mononucleosomal-sized and genomic DNA reference probes were prepared can be found in the Supplemental Experimental Procedures. Briefly, probe was prepared by micrococcal nuclease digestion of chromatin or genomic DNA, followed by T7 in vitro transcription linear amplification to synthesize aminoallyl-RNA probe that could be labeled for hybridization.

Analysis of Nucleosome Positions
Detailed explanations of data processing are presented in the supplemental methods. Final values for each tiling microarray probe were background median subtracted and normalized using a LOESS algorithm. Areas of nucleosome enrichment could be visualized using line traces connecting physically contiguous probes. Most data analysis used difference maps of nucleosome positions created by subtracting the log2 values of nucleosome positions of a control dataset from the corresponding positions in an experimental dataset. Prior to this transformation, nucleosome positions were aligned at the first nucleosome downstream of the NFR.

Chromatin Immunoprecipitation and QPCR
Chromatin immunoprecipitation and subsequent analysis by QPCR was performed as previously described (Raisner et al., 2005; Meneghini et al., 2003).

ACCESSION NUMBERS

Microarray data can be obtained from NCBI GEO at series accession GSE13446.

SUPPLEMENTAL DATA

Supplemental Data include Supplemental Experimental Procedures, Supplemental References, eight figures, and one table and can be found with this article online at http://www.cell.com/supplemental/S0092-8674(09)00257-8.

REFERENCES

Albert, I., Mavrich, T.N., Tomsho, L.P., Qi, J., Zanton, S.J., Schuster, S.C., and Pugh, B.F. (2007). Translational and rotational settings of H2A.Z nucleosomes across the Saccharomyces cerevisiae genome. Nature *446*, 572–576.

Angermayr, M., Oechsner, U., and Bandlow, W. (2003). Reb1p-dependent DNA bending effects nucleosome positioning and constitutive transcription at the yeast profilin promoter. J. Biol. Chem. *278*, 17918–17926.

Barski, A., Cuddapah, S., Cui, K., Roh, T.Y., Schones, D.E., Wang, Z., Wei, G., Chepelev, I., and Zhao, K. (2007). High-resolution profiling of histone methylations in the human genome. Cell *129*, 823–837.

Beinoraviciute-Kellner, R., Lipps, G., and Krauss, G. (2005). In vitro selection of DNA binding sites for ABF1 protein from Saccharomyces cerevisiae. FEBS Lett. *579*, 4535–4540.

Bernstein, B.E., Liu, C.L., Humphrey, E.L., Perlstein, E.O., and Schreiber, S.L. (2004). Global nucleosome occupancy in yeast. Genome Biol. 5, R62.

Buskirk, A.R., Ong, Y.C., Gartner, Z.J., and Liu, D.R. (2004). Directed evolution of ligand dependence: small-molecule-activated protein splicing. Proc. Natl. Acad. Sci. USA 101, 10505–10510.

Cairns, B.R., Lorch, Y., Li, Y., Zhang, M., Lacomis, L., Erdjument-Bromage, H., Tempst, P., Du, J., Laurent, B., and Kornberg, R.D. (1996). RSC, an essential, abundant chromatin-remodeling complex. Cell 87, 1249–1260.

Cairns, B.R., Schlichter, A., Erdjument-Bromage, H., Tempst, P., Kornberg, R.D., and Winston, F. (1999). Two functionally distinct forms of the RSC nucleosome-remodeling complex, containing essential AT hook, BAH, and bromo-domains. Mol. Cell 4, 715–723.

De Winde, J.H., Van Leeuwen, H.C., and Grivell, L.A. (1993). The multifunctional regulatory proteins ABF1 and CPF1 are involved in the formation of a nuclease-hypersensitive region in the promoter of the QCR8 gene. Yeast 9, 847–857.

Dohmen, R.J., and Varshavsky, A. (2005). Heat-inducible degron and the making of conditional mutants. Methods Enzymol. 399, 799–822.

Gavin, A.C., Bosche, M., Krause, R., Grandi, P., Marzioch, M., Bauer, A., Schultz, J., Rick, J.M., Michon, A.M., Cruciat, C.M., et al. (2002). Functional organization of the yeast proteome by systematic analysis of protein complexes. Nature 415, 141–147.

Guillemette, B., Bataille, A.R., Gevry, N., Adam, M., Blanchette, M., Robert, F., and Gaudreau, L. (2005). Variant Histone H2A.Z Is Globally Localized to the Promoters of Inactive Yeast Genes and Regulates Nucleosome Positioning. PLoS Biol. 3, e384.

Harbison, C.T., Gordon, D.B., Lee, T.I., Rinaldi, N.J., Macisaac, K.D., Danford, T.W., Hannett, N.M., Tagne, J.B., Reynolds, D.B., Yoo, J., et al. (2004). Transcriptional regulatory code of a eukaryotic genome. Nature 431, 99–104.

Ioshikhes, I.P., Albert, I., Zanton, S.J., and Pugh, B.F. (2006). Nucleosome positions predicted through comparative genomics. Nat. Genet. 38, 1210–1215.

Jakobovits, E.B., Bratosin, S., and Aloni, Y. (1980). A nucleosome-free region in SV40 minichromosomes. Nature 285, 263–265.

Lam, F.H., Steger, D.J., and O'Shea, E.K. (2008). Chromatin decouples promoter threshold from dynamic range. Nature 453, 246–250.

Lee, W., Tillo, D., Bray, N., Morse, R.H., Davis, R.W., Hughes, T.R., and Nislow, C. (2007). A high-resolution atlas of nucleosome occupancy in yeast. Nat. Genet. 39, 1235–1244.

Li, B., Pattenden, S.G., Lee, D., Gutierrez, J., Chen, J., Seidel, C., Gerton, J., and Workman, J.L. (2005). Preferential occupancy of histone variant H2AZ at inactive promoters influences local histone modifications and chromatin remodeling. Proc. Natl. Acad. Sci. USA 102, 18385–18390.

Liaw, P.C., and Brandl, C.J. (1994). Defining the sequence specificity of the Saccharomyces cerevisiae DNA binding protein REB1p by selecting binding sites from random-sequence oligonucleotides. Yeast 10, 771–787.

Lorch, Y., Zhang, M., and Kornberg, R.D. (2001). RSC unravels the nucleosome. Mol. Cell 7, 89–95.

Mavrich, T.N., Ioshikhes, I.P., Venters, B.J., Jiang, C., Tomsho, L.P., Qi, J., Schuster, S.C., Albert, I., and Pugh, B.F. (2008a). A barrier nucleosome model for statistical positioning of nucleosomes throughout the yeast genome. Genome Res. 18, 1073–1083.

Mavrich, T.N., Jiang, C., Ioshikhes, I.P., Li, X., Venters, B.J., Zanton, S.J., Tomsho, L.P., Qi, J., Glaser, R.L., Schuster, S.C., et al. (2008b). Nucleosome organization in the Drosophila genome. Nature 453, 358–362.

Meneghini, M.D., Wu, M., and Madhani, H.D. (2003). Conserved histone variant H2A.Z protects euchromatin from the ectopic spread of silent heterochromatin. Cell 112, 725–736.

Nagalakshmi, U., Wang, Z., Waern, K., Shou, C., Raha, D., Gerstein, M., and Snyder, M. (2008). The transcriptional landscape of the yeast genome defined by RNA sequencing. Science 320, 1344–1349.

Ng, H.H., Robert, F., Young, R.A., and Struhl, K. (2002). Genome-wide location and regulated recruitment of the RSC nucleosome-remodeling complex. Genes Dev. 16, 806–819.

Nonet, M., Scafe, C., Sexton, J., and Young, R. (1987). Eucaryotic RNA polymerase conditional mutant that rapidly ceases mRNA synthesis. Mol. Cell. Biol. 7, 1602–1611.

Ozsolak, F., Song, J.S., Liu, X.S., and Fisher, D.E. (2007). High-throughput mapping of the chromatin structure of human promoters. Nat. Biotechnol. 25, 244–248.

Parnell, T.J., Huff, J.T., and Cairns, B.R. (2008). RSC regulates nucleosome positioning at Pol II genes and density at Pol III genes. EMBO J. 27, 100–110.

Peckham, H.E., Thurman, R.E., Fu, Y., Stamatoyannopoulos, J.A., Noble, W.S., Struhl, K., and Weng, Z. (2007). Nucleosome positioning signals in genomic DNA. Genome Res. 17, 1170–1177.

Raisner, R.M., Hartley, P.D., Meneghini, M.D., Bao, M.Z., Liu, C.L., Schreiber, S.L., Rando, O.J., and Madhani, H.D. (2005). Histone variant H2A.Z marks the 5′ ends of both active and inactive genes in euchromatin. Cell 123, 233–248.

Reed, S.H., Akiyama, M., Stillman, B., and Friedberg, E.C. (1999). Yeast autonomously replicating sequence binding factor is involved in nucleotide excision repair. Genes Dev. 13, 3052–3058.

Saragosti, S., Moyne, G., and Yaniv, M. (1980). Absence of nucleosomes in a fraction of SV40 chromatin between the origin of replication and the region coding for the late leader RNA. Cell 20, 65–73.

Schones, D.E., Cui, K., Cuddapah, S., Roh, T.Y., Barski, A., Wang, Z., Wei, G., and Zhao, K. (2008). Dynamic regulation of nucleosome positioning in the human genome. Cell 132, 887–898.

Segal, E., Fondufe-Mittendorf, Y., Chen, L., Thastrom, A., Field, Y., Moore, I.K., Wang, J.P., and Widom, J. (2006). A genomic code for nucleosome positioning. Nature 442, 772–778.

Segal, M. R. (2008). Re-cracking the nucleosome positioning code. Stat. Appl. Genet. Mol. Biol. 7, Article14.

Shivaswamy, S., Bhinge, A., Zhao, Y., Jones, S., Hirst, M., and Iyer, V.R. (2008). Dynamic remodeling of individual nucleosomes across a eukaryotic genome in response to transcriptional perturbation. PLoS Biol. 6, e65.

Storici, F., Durham, C.L., Gordenin, D.A., and Resnick, M.A. (2003). Chromosomal site-specific double-strand breaks are efficiently targeted for repair by oligonucleotides in yeast. Proc. Natl. Acad. Sci. USA 100, 14994–14999.

Whitehouse, I., Rando, O.J., Delrow, J., and Tsukiyama, T. (2007). Chromatin remodelling at promoters suppresses antisense transcription. Nature 450, 1031–1035.

Whitehouse, I., and Tsukiyama, T. (2006). Antagonistic forces that position nucleosomes in vivo. Nat. Struct. Mol. Biol. 13, 633–640.

Yang, J.G., Madrid, T.S., Sevastopoulos, E., and Narlikar, G.J. (2006). The chromatin-remodeling enzyme ACF is an ATP-dependent DNA length sensor that regulates nucleosome spacing. Nat. Struct. Mol. Biol. 13, 1078–1083.

Yang, Y.H., Dudoit, S., Luu, P., Lin, D.M., Peng, V., Ngai, J., and Spped, T.P. (2002). Normalization for cDNA microarray data: a robust composite method addressing single and multiple slide systemic variation. Nucleic Acids Res. 30, e15.

Yuan, G.C., and Liu, J.S. (2008). Genomic sequence is highly predictive of local nucleosome depletion. PLoS Comput Biol 4, e13.

Yuan, G.C., Liu, Y.J., Dion, M.F., Slack, M.D., Wu, L.F., Altschuler, S.J., and Rando, O.J. (2005). Genome-scale identification of nucleosome positions in S. cerevisiae. Science 309, 626–630.

Zanton, S.J., and Pugh, B.F. (2006). Full and partial genome-wide assembly and disassembly of the yeast transcription machinery in response to heat shock. Genes Dev. 20, 2250–2265.

Zhang, H., Roberts, D.N., and Cairns, B.R. (2005). Genome-wide dynamics of Htz1, a histone H2A variant that poises repressed/basal promoters for activation through histone loss. Cell 123, 219–231.

Zilberman, D., Coleman-Derr, D., Ballinger, T., and Henikoff, S. (2008). Histone H2A.Z and DNA methylation are mutually antagonistic chromatin marks. Nature 456, 125–129.

Cell